INSTITUTE FOR HIGH ENERGY PHYSICS

IHEP 93-63
OMMC

A.V.Kostritskii, L.O. Baliev, A.F. Buzulutskov,
A.O.Efimov, V.I.Kryshkin, A.V.Levin, S.A.Nikitin

SCINTILLATING PADDLE/FIBER HADRON CALORIMETER

Submitted to *PTE, NIM*

Protvino 1993

UDK 539.1.083.91 M-24

Abstract

Kostritskii A.V. et al. Scintillating paddle/fiber hadron calorimeter: IHEP Preprint 93-63. – Protvino, 1993. – p. 12, figs. 12, refs.: 1.

A hadron calorimeter in which the scintillator paddles are placed parallel to particle trajectories and light is collected by optical fibers with WLS is described. The active element of the calorimeter is studied and the performance of the calorimeter in typical collider environment is simulated. A design of the calorimeter module is presented.

Аннотация

Кострицкий А.В. и др. Адронный калориметр с переизлучающими волокнами: Препринт ИФВЭ 93-63. – Протвино, 1993. – 12 с., 12 рис., библиогр.: 1.

Описывается проект адронного калориметра, в котором сцинтилляторы расположены параллельно пучку частиц, а светосбор со сцинтилляторов осуществляется оптическими волокнами с переизлучателем. Проведены исследования активного элемента калориметра и моделирование работы калориметра в условиях, типичных для коллайдерных установок. Приводится конструкция модуля калориметра.

1. Introduction

In [1] a hadron calorimeter has been proposed which is simple to construct, easy to assemble and has no dead space. In this article we consider several types of the active element (scintillator/WLS fiber) and simulate the calorimeter performance in typical collider environment. A design of the module is proposed.

2. The active element

The gist of the proposed construction (see fig. 1) consists in placing scintillators interspersed with absorbers almost parallel to the beam particles. Optical fibers with WLS are applied to the narrow edges of the scintillator paddles. The fibers are bundled together and coupled to a photodetector.

Fig. 2 presents the active element structure of the hadron calorimeter. The scintillator is divided into two parts to measure the longitudinal shower development. Obviously, the scintillator can be divided into more parts viewed by a single fiber which can be useful in case of production of the scintillators by molding. The scintillators have trapezoid shape for projecting geometry. Two methods of light collection were studied . Fig. 2a illustrates the first one. A fiber with WLS is embedded in a grove 1.3 mm wide and 1.3 mm deep machined in the first scintillator and 2.6 mm deep in the second one. In the other method, shown in fig. 2b, the fibers are put to the edges of the scintillators and only at the end of the second scintillator the fibers are inserted into a grove to bend them close to the back side of the tower. The section of the fibers from the first part of the scintillator is painted black to isolate them from the second scintillator. Without the light isolation the first fiber will collect the total light from a calorimeter (to be used for a trigger) and the other fiber - from the

second part. On the back side of the calorimeter the fibers are laid out in a pattern shown in fig. 3 and coupled to photodetectors or to clear fibers to guide the light outside of the magnetic field. It is easy to couple both ends to a single photodetector but the use of two photodetectors can be preferable to eliminate the cases of shower debris passing through the photodetector. To measure the efficiency of the light collection there was made a 4 mm thick scintillating element with dimensions presented in fig. 2. The 1.2 mm diameter fiber was doped with K-27. The polystyrene core and cladding material of the fiber had refractive indices of $n_1 = 1.59$ and $n_2 = 1.39$, respectively. Both fibers were air coupled to a photomultiplier FEU-85. On the opposite fibre ends (for the case in fig. 2a) a reflective aluminum layer was deposited under vacuum providing 50% reflectivity. The scintillators were wrapped into aluminized mylar. The number of photoelectrons (p.e.) was measured with two scintillator counters to trigger on passage of electron from Ru^{106}. For both methods (2a and 2b) it was equal to $N_{p.e} = 3.0$.

Quantum sensitivity of a silicon photodiode is about an order of magnitude higher than that of FEU-85. One can estimate the level of amplitude signal from muon passage through the calorimeter with a silicon photodiode as a photodetector. For 4 mm thick scintillator and absorber/scintillator thickness ratio 4:1 the muon path in scintillator (95 cm long calorimeter) is 19 cm. Then the number of detected electrons will be about 1425.

3. Simulation of the calorimeter performance

The proposed calorimeter is vulnerable to "channeling" (similar to spaghetti type calorimeters) when a particle hits the scintillator and goes a long way without interaction. The cure for the effect is well known - the calorimeter must be tilted relative to the particle beam. But the presence of magnetic field makes this angle dependent on the particle momentum and charge sign. On the other hand, an electromagnetic calorimeter about one interaction length is placed in front of the hadron calorimeter, as a rule. To study the performance of the calorimeter for different setups a simulation was done with GEANT. In all calculations the absorber plates had a wedge form (see fig. 10).

Fig. 4 gives the calorimeter energy resolution as a function of the angle θ_z between the calorimeter axis and a particle trajectory under the following assumptions:

1. No matter in front of the hadron calorimeter, magnetic field is zero. One can see a sharp angular dependence of the energy resolution impaired by the longitudinal leakage

2. An electromagnetic calorimeter of 1.6 interaction lengths made of CF_3 is placed in front of the hadron calorimeter, magnetic field is zero. The energy released in the electromagnetic and hadron calorimeters is summed up. The angular dependence becomes significantly weaker and the energy resolution is improved due to fuller containment of the shower.

3. An electromagnetic calorimeter of 1.6 interaction lengths is placed in front of the hadron calorimeter, magnetic field is 4 Tesla. In a wide angular range the energy resolution is constant.

The calorimeter consists of 95 cm long copper plates 3 mm thick in front and 5 mm thick at back interspersed with scintillator plates 2.5 mm thick (constant thickness). The incident particles (protons) momentum is 10 GeV/c to minimize the longitudinal leakage. A calculation has been carried out with scintillator thickness of which varied from 2 mm to 3.5 mm, i.e. the absorber/scintillator ratio was constant along the depth. The energy resolution improved from 60% to 55%. It is more practical to realize this condition not by scintillator in the form of a wedge but variation of light collection efficiency from the scintillator in depth proportional to the absorber thickness variation (for example, putting a black paper in the form of a wedge on the scintillator).

Fig. 5 shows the energy resolution dependence on the copper plate thickness (at the calorimeter entrance). The scintillator thickness was 2.5 mm, there was an electromagnetic calorimeter of 1.6 absorption lengths in front of the hadron one, the particle trajectory angle was 5° and no magnetic field.

Fig. 6 presents the energy resolution dependence on particle energy (with 1.6 interaction lengths electromagnetic calorimeter in front of the hadron calorimeter, magnetic field is 4 Tesla). The 95 cm long copper plates were 10 mm thick at the entrance and the scintillator plates were 2.5 mm thick. The resolution degradation with the particle energy is due to the energy leakage through the backside. For a 40 interaction length calorimeter with the same absorber thickness at the entrance the energy resolution is well described by expression $\sigma/E = 54\%/\sqrt{E} \oplus 7.8\%$ in the energy range 10-100 GeV. In this case the variation of the light collection efficiency from the scintillator in depth was proportional to the absorber thickness variation. If in such calorimeter the energy released in the absorber and in the scintillator (without variation of the light collection efficiency) is summed up ("ideal" calorimeter) the energy resolution is described by expression $\sigma/E = 38\%/\sqrt{E} \oplus 5.5\%$.

For the next generation collider the typical radiation length of an electromagnetic calorimeter placed in front of a hadron one is about 25 X_0. With the growth of particle energy (electron or photon) the longitudinal leakage will lead to a detrimental effect on the electromagnetic calorimeter resolution. Measure-

ment by hadron calorimeter of the escaping part of the electromagnetic shower ameliorates the resolution. Fig. 7 illustrates the energy dependence of the electromagnetic calorimeter resolution (25 X_0) on electron energy without summing the amplitudes from the hadron calorimeter and with summing. The energy resolution of the electromagnetic calorimeter was taken as $\sigma/E = 2\%/\sqrt{E}$ for full containment of electromagnetic shower. The copper was 10 mm thick, the scintillator was 2.5 mm thick and the calorimeter was tilted by 5°. The hadron calorimeter was supposed to have no energy threshold. Fig. 8 shows the combined energy resolution versus the energy threshold of the hadron calorimeter.

4. Design of the calorimeter module

The main advantage of the proposed calorimeter is possibility to use the absorbers as the support structure for the barrel calorimeter. Fig. 9 shows the cut-out view of the module. The wedge absorbers with the same cross section for all central calorimeters (see fig. 10) have small projections to fasten adjacent plates. The layout of the module is presented in fig. 11. The absorber plates are fastened through spacers, whose thickness is equal to the scintillator thickness. Fig. 12 shows the scintillator paddles with WLS fibers put on the front and back surfaces of the calorimeter (for longitudinal division into two parts). The number of photoelectrons for this configuration (perpendicular passage of particle through the scintillator) was also 3.

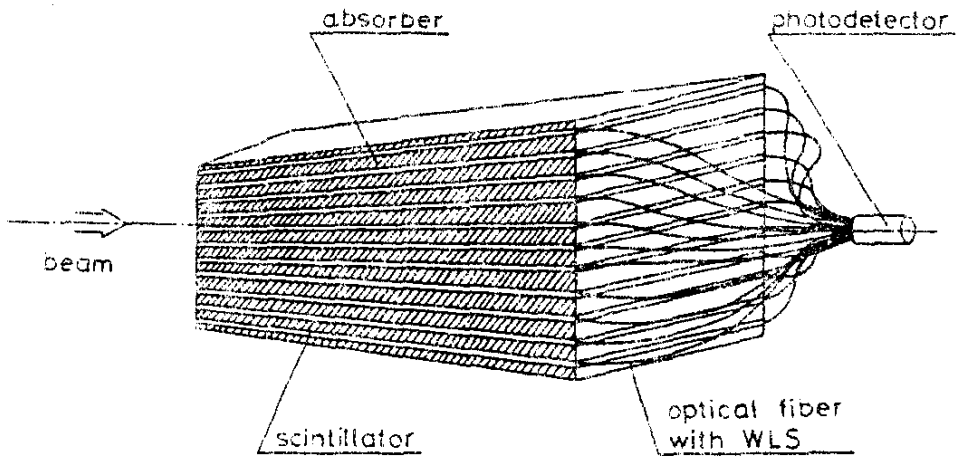

Figure 1. Schematic view of the calorimeter.

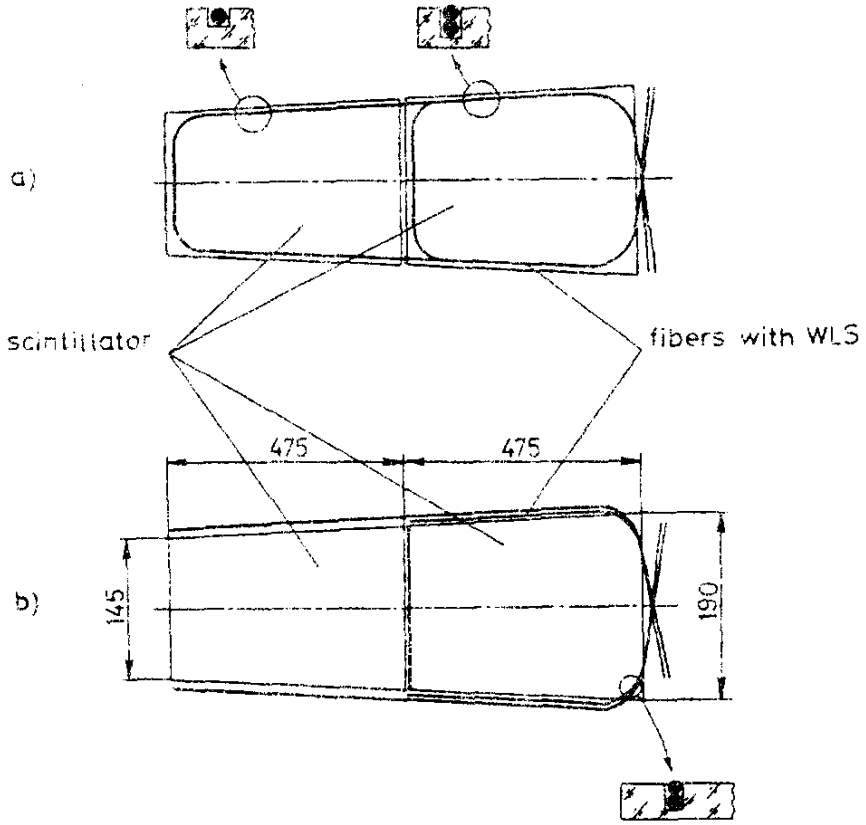

Figure 2. Scintillating paddle/fiber assembly.

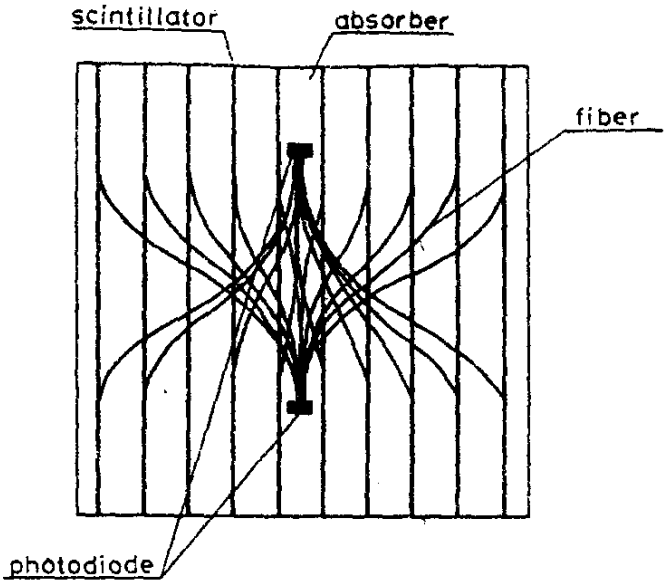

Figure 3. Arrangement of fibers outside of the calorimeter to minimize the gap between the calorimeter and a magnetic coil.

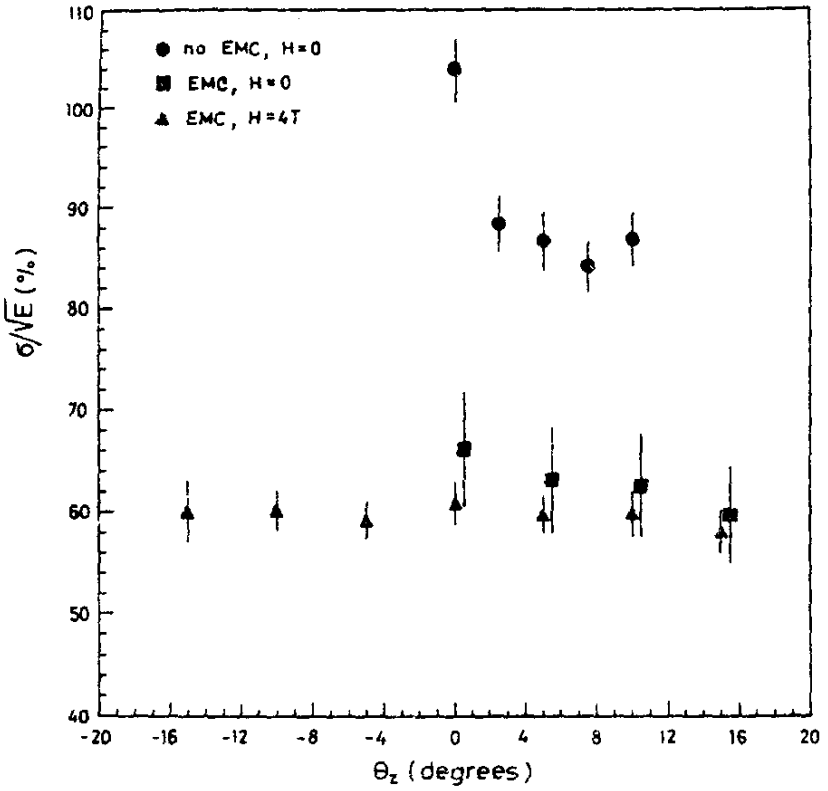

Figure 4. The energy dependence on angle for different conditions: a) without electromagnetic calorimeter and without magnetic field ; b) with electromagnetic calorimeter of 1.6 absorption lengths and without magnetic field; c) with electromagnetic calorimeter and magnetic field 4 T.

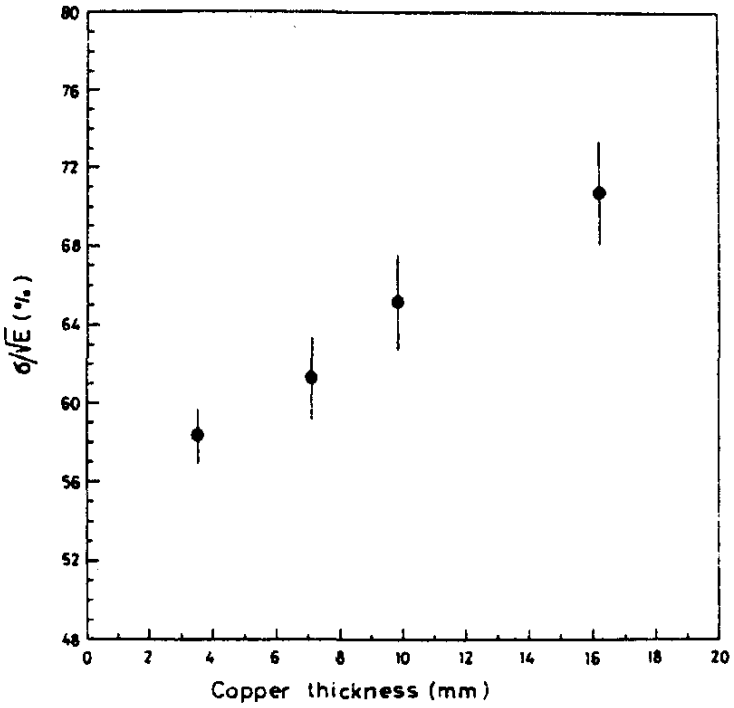

Figure 5. The energy dependence on the copper absorber thickness.

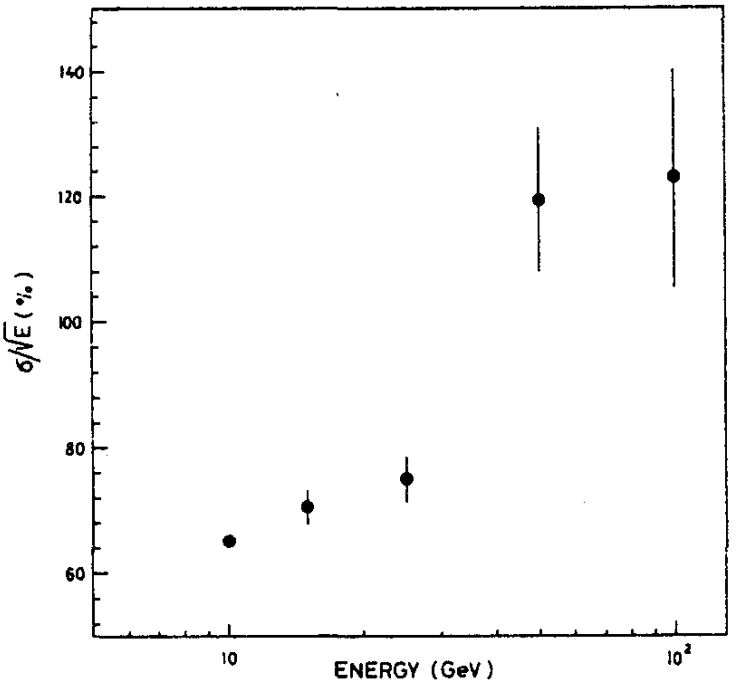

Figure 6. The energy dependence on particle energy.

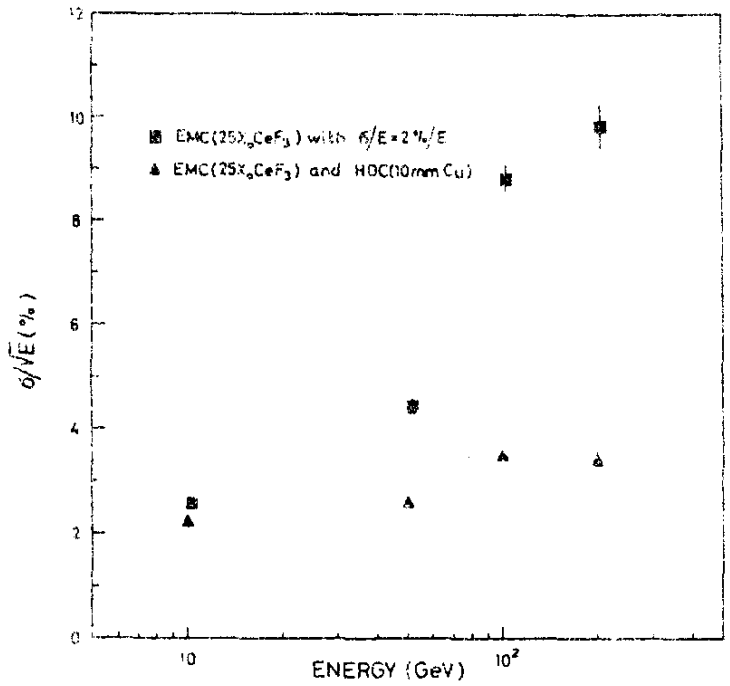

Figure 7. The energy resolution of a 25 X_0 electromagnetic calorimeter versus electron energy without summing energy from hadron calorimeter and with summing.

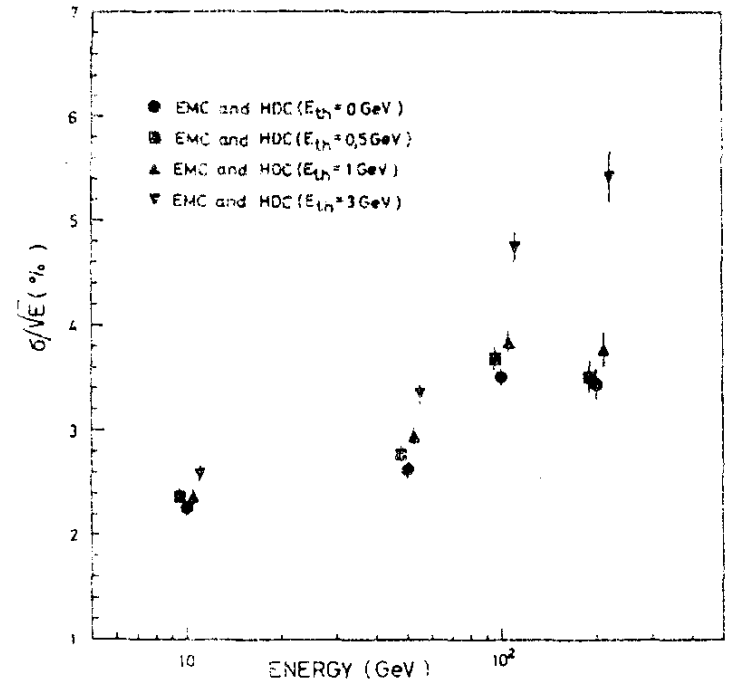

Figure 8. The energy resolution of a 25 X_0 electromagnetic calorimeter versus electron energy with summing energy from the hadron calorimeter without energy threshold and with 0.5 - 3 GeV energy threshold.

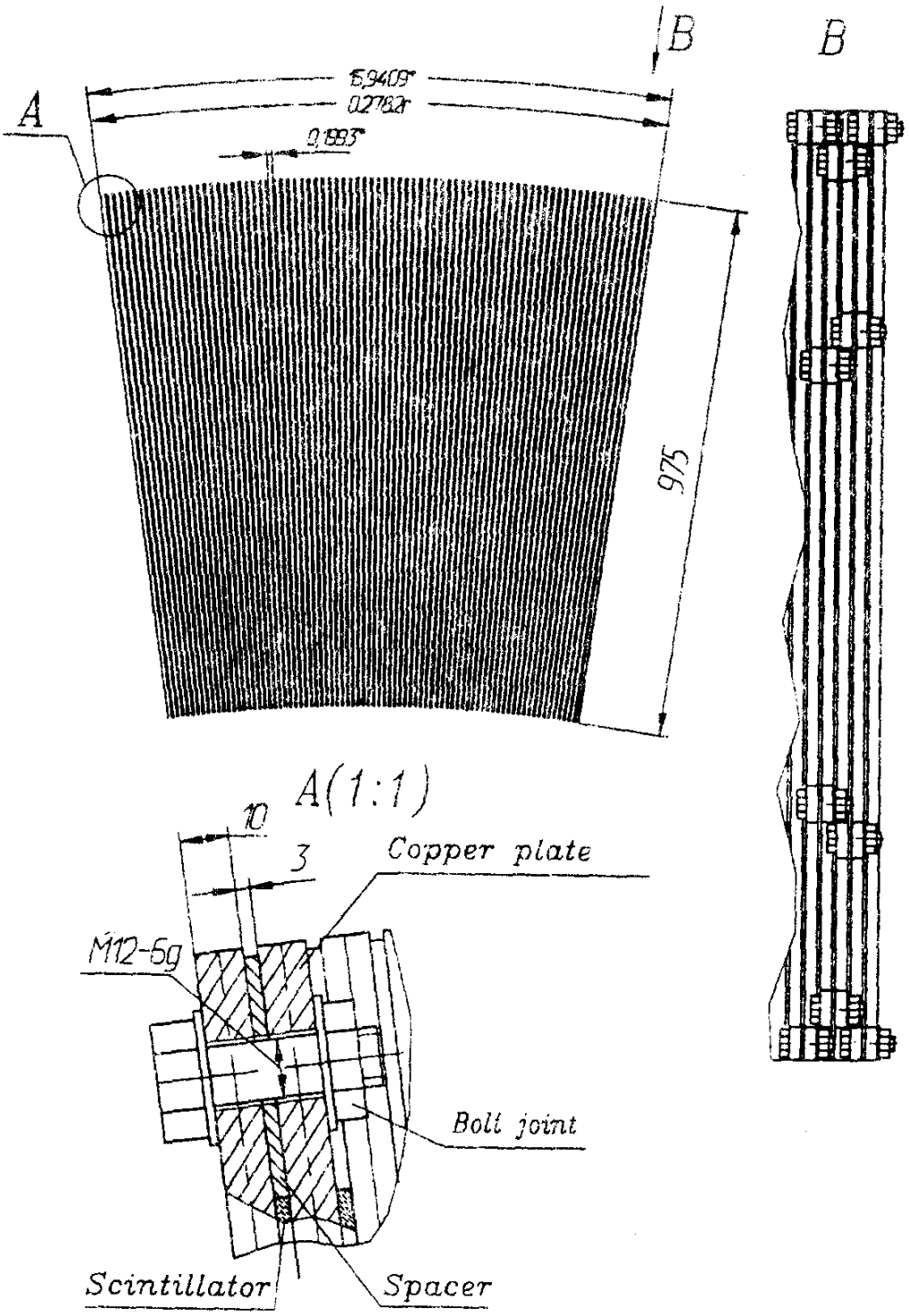

Figure 9. Cut-out view of the barrel calorimeter module.

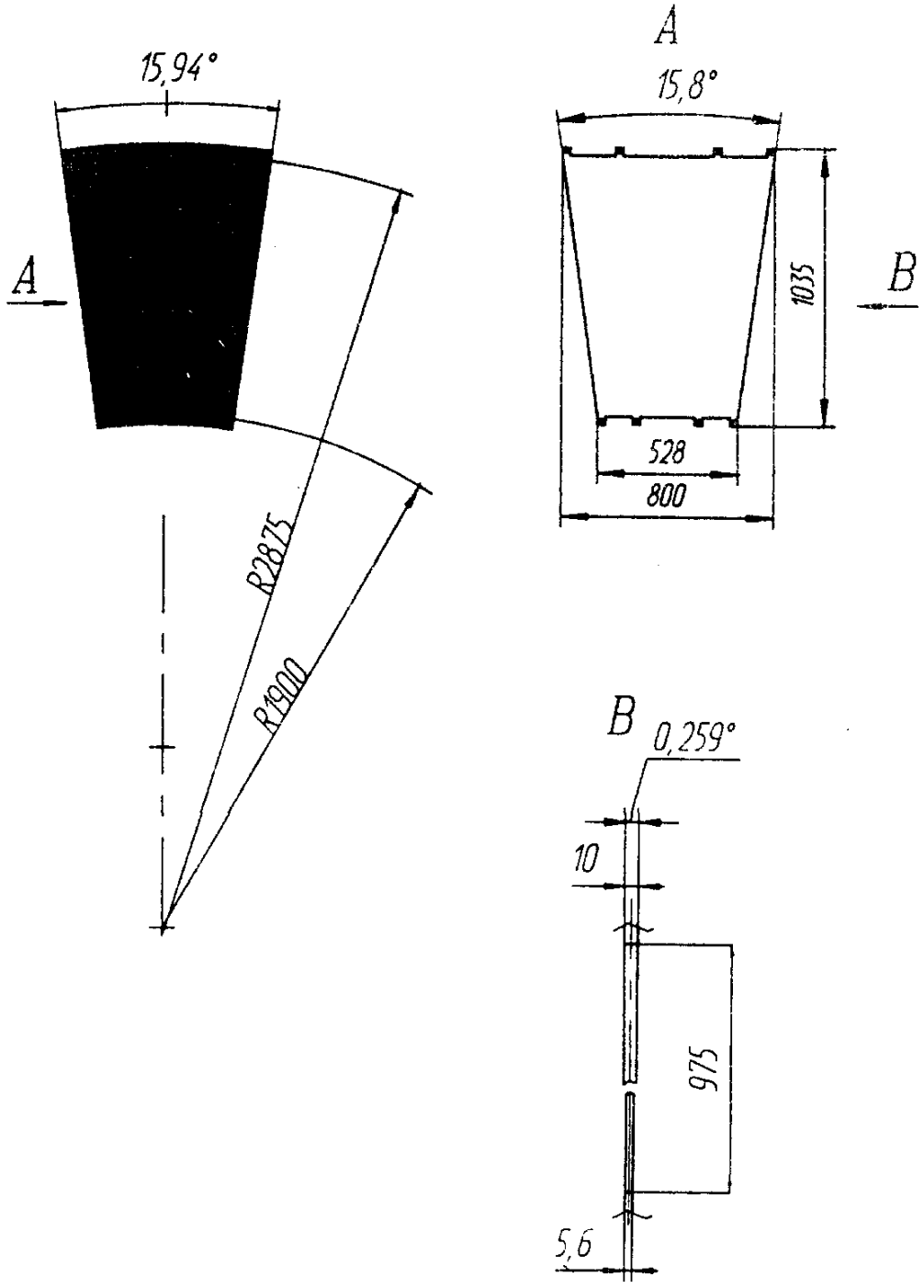

Figure 10. Absorber plates.

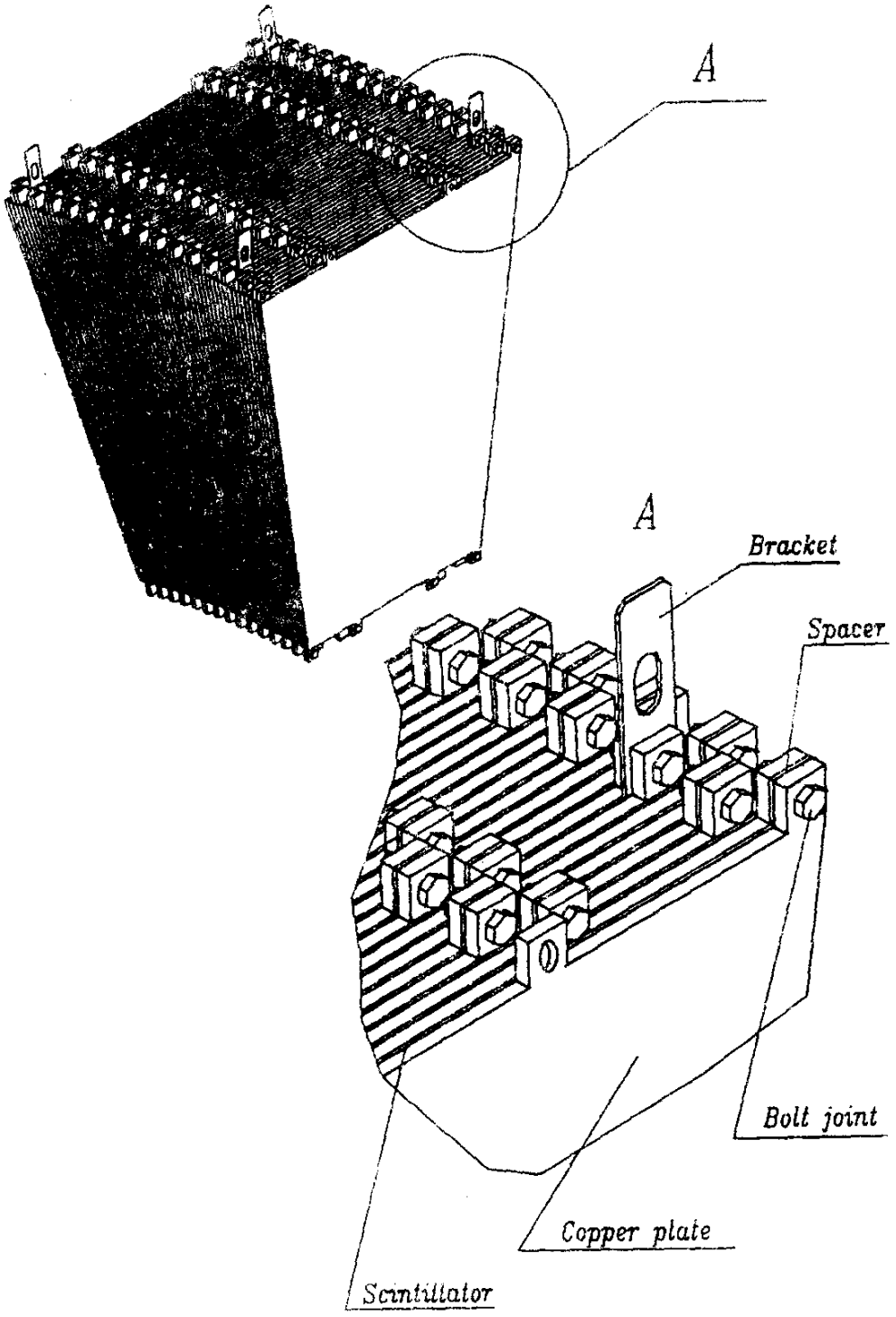

Figure 1: View of the barrel calorimeter module.

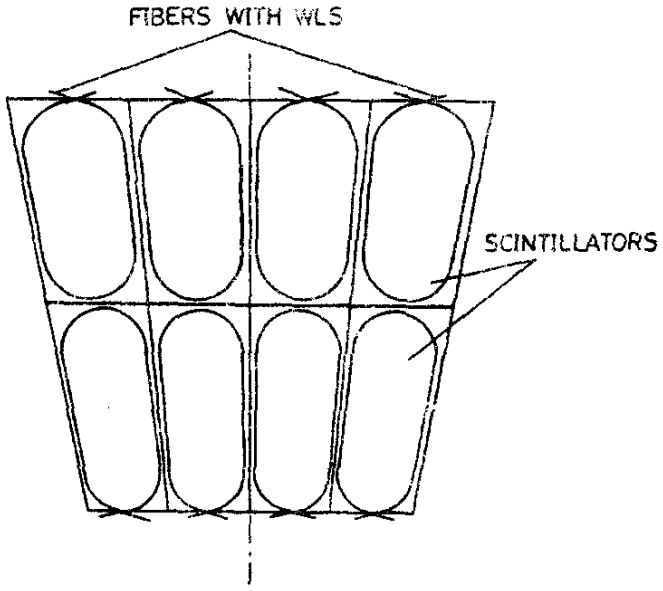

Figure 12. The layer of the scintillator paddles with WLS fibers.

5. Conclusion

In conclusion we summarize the results:

-a construction of active element is proposed which easily allows to make longitudinal division, requires small space for photodetectors, easy to produce and assemble;

-because all scintillators end at the flanges of the calorimeter it is simply to realize a control of active element performance with a radioactive source;

-calculations show that for typical collider conditions (the electromagnetic calorimeter in front of the hadron calorimeter, magnetic field) the channeling is not a serious problem even for a single particle, the effect will be further suppressed for jets;

-the absorber thickness is 1.4 cm for the energy resolution $\sigma/E = 70\%/\sqrt{E}$;

-the proposed design of the module for a barrel calorimeter does not need additional support structure that excludes dead zones.

References

[1] Kryshkin V.I., Lapshin V.G., Mysnik A.I. et al.- Preprint IHEP 92-95.- Protvino, 1992.

Received April 26, 1993

А.В.Кострицкий и др.
Адронный калориметр с переизлучающими волокнами.

Оригинал-макет подготовлен с помощью системы LaTeX.
Редактор А.А.Антипова. Технический редактор Л.П.Тимкина.
Корректор Е.Н.Горина.

Подписано к печати 28.04.1993г. Формат 60 × 90/16.
Офсетная печать. Печ.л. 0,75. Уч.-изд.л. 0,94. Тираж 260.
Заказ 816. Индекс 3649. Цена 49 руб.

Институт физики высоких энергий, 142284, Протвино Московской обл.

49 руб. Индекс 3649

П Р Е П Р И Н Т 93-63, И Ф В Э, 1993